Journal of Quantitative Spectroscopy & Radiative Transfer 179 (2016) 1–10

Contents lists available at ScienceDirect

Journal of Quantitative Spectroscopy & Radiative Transfer

journal homepage: www.elsevier.com/locate/jqsrt

Rigorous 3-D vectorial complex ray model applied to light scattering by an arbitrary spheroid

Bingqiang Sun [a,*], George W. Kattawar [b], Ping Yang [c,a], Kuan Fang Ren [d]

[a] Department of Physics & Astronomy, Texas A&M University, College Station, TX 77843, USA
[b] Department of Physics & Astronomy and Institute for Quantum Science and Engineering, Texas A&M University, College Station, TX 77843, USA
[c] Department of Atmospheric Sciences, Texas A&M University, College Station, TX 77843, USA
[d] CORIA-UMR6614, Normandie Université, CNRS, Université et INSA de Rouen Av de l'Université, 76800 Saint Etienne du Rouvray, France

ARTICLE INFO

Article history:
Received 24 December 2015
Received in revised form
4 March 2016
Accepted 4 March 2016
Available online 11 March 2016

Keywords:
Light scattering
Vectorial complex ray-tracing
Spheroid

ABSTRACT

After a ray bundle passes a curved surface, the equal-phase wavefront associated with the refracted rays will be distorted. Consequently, the cross-section of a ray bundle with a curved wavefront during propagation in a homogeneous medium will vary with the ray-bundle propagation distance. Moreover, the phase of a ray bundle with convergent wavefront will undergo a phase shift of $\pi/2$ with each passage of a focal line. The contribution to the scattering amplitude by a ray bundle after passing a scatterer is determined by three elements: the cross-section variation of its wavefront, the total phase, and the refraction coefficients determined by Fresnel equations. In the geometric optics regime, the aforesaid three elements caused by a curved surface can be systematically quantified in terms of the vectorial complex ray-tracing technique. In this study, rigorous vectorial complex ray-tracing calculations are conducted for light scattering by a general spheroid and the results are validated in comparison with the benchmarks provided by the rigorous T-matrix method.

1. Introduction

The single-scattering properties of homogeneous spheres or multiple spherical shells for given sizes can be analytically obtained by the Lorenz–Mie theory [1,2]. Light scattering by small-sized arbitrary scatterers can be modeled by numerically accurate methods including the discrete dipole approximation method (DDA) [3–5], finite difference time domain method (FDTD) [6–8], and pseudo-spectral time domain method (PSTD) [9–11]. For small-to-moderate scatterers with rotational symmetry, two effective realizations of the T-matrix method, namely, the extended boundary condition method (EBCM) [12–14] and invariant-imbedding T-matrix method (IITM) [15,16], can facilitate the single-scattering property computations much more accurately and effectively than numerical methods, particularly in the case of randomly oriented particles. For a scatterer with its characteristic dimension much larger than the incident wavelength, the geometric optics method can provide a reasonably accurate approximation [17–19]. In some geometric optics methods, the physical-optics effect, such as accurately mapping the near-field to far-field (e.g. [18]), surface waves (e.g. [20]), tunneling rays (e.g. [21]), and, caustics (e.g. [22]), has been taken into consideration.

For a scatterer with a curved surface, the wavefront of a refracted wave is distorted. Compared to the conventional geometric optics method, a divergence factor must be introduced to represent the effect caused by wavefront distortion [1,20,23–25]. Consequently, the variations in the phase and cross-section of a ray bundle will give rise to additional complexity in comparison with ray tracing in

* Corresponding author.
E-mail address: bqsun@physics.tamu.edu (B. Sun).

http://dx.doi.org/10.1016/j.jqsrt.2016.03.010
0022-4073/

the case of a scatterer with facet faces [1,26]. The effect caused by wavefront distortion has been theoretically and experimentally studied using the vectorial complex ray model in 2D propagation where the incident and refracted rays remain in the same plane [25,27–29]. In this study, the vectorial complex ray-tracing technique [22] including the wavefront distortion effect is implemented for the 3D case for a general spheroid; however, the present study is still restricted to the pure geometric optics method.

The present study focuses on the scattering phase matrix, which includes all the scattering information and can be obtained from the amplitude scattering matrix [1,2,14]. The amplitude scattering matrix **S** defined with respect to the scattering plane spanned by the incident and scattered directions shown in Fig. 1 is given in the form [1,2]:

$$\begin{pmatrix} E_{\parallel}^{\mathrm{sca}} \\ E_{\perp}^{\mathrm{sca}} \end{pmatrix} = \frac{\exp(ikr)}{-ikr} \begin{pmatrix} S_{11} & S_{12} \\ S_{21} & S_{22} \end{pmatrix} \begin{pmatrix} E_{\parallel}^{\mathrm{inc}} \\ E_{\perp}^{\mathrm{inc}} \end{pmatrix} \tag{1}$$

where r is the distance from the origin to the point of observation; The quantities $E_{\parallel}$ and $E_{\perp}$ are the parallel and perpendicular components of the electric field, decomposed with respect to the scattering plane. The superscripts "inc" and "sca" denote the incident and scattered quantities.

2. Method

2.1. Scattering amplitude

Consider a scatterer of refractive index m illuminated by a plane wave with wavelength λ, and assume a ray bundle with a plane wavefront to impinge on the surface of the scatterer with a solid angle element $d\Omega_{\mathrm{int}}$, which is defined in terms of the area of the image of a Gauss map of the corresponding incident area. Consequently, a scattered ray bundle will spread into a solid angle $d\Omega_{\mathrm{sca}}$, which is defined as the area of the image of a Gauss map of the corresponding wavefront [30]. The intensity of the scattered light can be formulated as [1]:

$$I_S = T_f I_0 \frac{\cos\,\theta_{i,1} d\Omega_{\mathrm{int}}/K_{\mathrm{int}}}{d\Omega_{\mathrm{sca}}/K_{\mathrm{sca}}} \tag{2}$$

where I_0 and I_S are respectively the incident and scattered intensities; K_{int} and K_{sca} are the Gaussian curvatures of the surface of the scatterer at the incident point and the wavefront of the scattered light, respectively; $\theta_{i,1}$ is the initial incident angle. The transmission coefficients T_f are related to the Fresnel equations and incident and refracted angles by

$$T_{f,p} = \begin{cases} |r_1|^2, & p = 0 \\ \left(\frac{\cos\,\theta_{t,p+1}}{\cos\,\theta_{i,p+1}}|t_{p+1}|^2\right)\left(\left|\prod_{n=2}^{p} r_n\right|^2\right)\left(\frac{\cos\,\theta_{t,1}}{\cos\,\theta_{i,1}}|t_1|^2\right), & p \geq 1 \end{cases} \tag{3}$$

where the subscript p is the order of the emergent ray (Fig. 2), r_n and t_n are respectively the Fresnel reflection and refraction coefficients at the n^{th} interaction of the ray with the particle surface. $\theta_{i,n}$ and $\theta_{t,n}$ are the incident angle and the refracted angle of the n^{th} interaction of the ray with the particle surface. In the far field, the scattering wave is spherical, $K_{\mathrm{sca}} = 1/r^2$, and the scattering matrix for a ray bundle can be formulated in the form:

$$\mathbf{S} = \sum_{p=0}^{\infty} \exp(i\zeta_p)\sqrt{D_p}\mathbf{U_p}\mathbf{G} \tag{4}$$

where ζ_p is the phase of the scattered wave, which consists of the phase shift due to the length of optical path relative to the reference ray, the dot-dashed line in Fig. 2, and the phase shift due to the focal points/lines [1]; $\mathbf{U_p}$ is a coefficient matrix, which is related to the Fresnel coefficients and the corresponding rotation matrices. $\mathbf{G}$ is a rotation matrix related to the incident frame of reference and the scattering plane defined by [31]:

$$G = \begin{pmatrix} \hat{e}_Y \cdot \hat{e}_{\parallel}^{\mathrm{int}} & \hat{e}_Y \cdot \hat{e}_{\perp}^{\mathrm{int}} \\ \hat{e}_X \cdot \hat{e}_{\parallel}^{\mathrm{int}} & \hat{e}_X \cdot \hat{e}_{\perp}^{\mathrm{int}} \end{pmatrix} \tag{5}$$

where the $\hat{e}_X$ and $\hat{e}_Y$ represent the unit vectors along X-axis and Y-axis directions in the incident frame of reference and, $\hat{e}_{\parallel}^{\mathrm{int}}$ and $\hat{e}_{\perp}^{\mathrm{int}}$ the unit vectors parallel and perpendicular to the scattering plane, as shown in Fig. 1. The divergence factor is defined by [1,25]:

$$D_p = \frac{\cos\,\theta_{t,p+1}\,\cos\,\theta_{t,1}}{\cos\,\theta_{i,p+1}} \frac{d\Omega_{\mathrm{int}}/K_{\mathrm{int}}}{d\Omega_{\mathrm{sca}}} = \frac{1}{K_{t,1}} \prod_{n=2}^{p+1} \frac{K_{i,n}}{K_{t,n}} \tag{6}$$

where $K_{i,n}$ and $K_{t,n}$ are respectively the corresponding Gaussian curvature of the wavefront of the incident and refracted rays at the n^{th} interaction of the ray with the particle surface. The total scattering matrix associated with

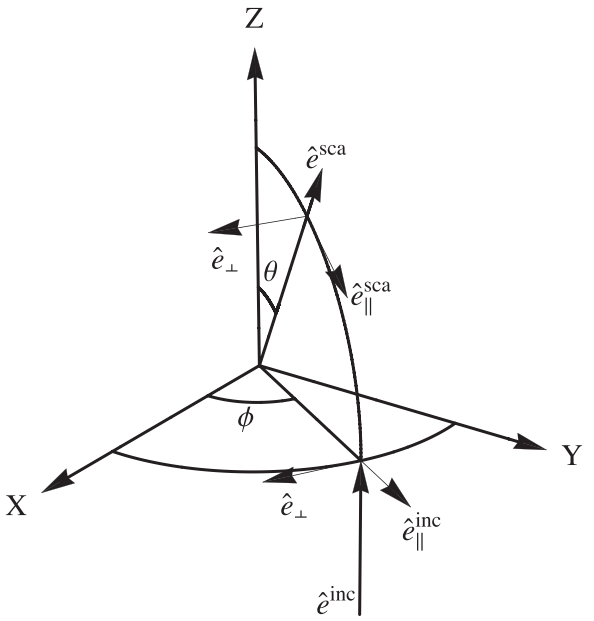

Fig. 1. Scattering plane spanned by the incident and scattered directions, i.e., $\hat{e}^{inc}$ and $\hat{e}^{sca}$, in the incident frame of reference, where the incident direction is along the z-axis. θ and ϕ are the zenith and azimuthal angles in the incident frame of reference. The subscripts $\parallel$ and $\perp$ are the corresponding parallel and perpendicular components with respect to the scattering plane, respectively.